104151
#1

Phase I Final Report

Development of Single Pass Drilling Technology through Investigations in Drilling Burr Elimination

5/15/2007

By

Thomas R. Newton

John Morehouse

Dr. Shreyes N. Melkote

George W. Woodruff School of Mechanical Engineering

Georgia Institute of Technology

801 Ferst Drive, Atlanta, Georgia 30332-0405

Executive Summary

Interfacial burr formation in the drilling of stacked sheets of material is a common problem in aircraft structure assembly. Eliminating or minimizing interfacial burrs may prevent the current need for de-stacking and deburring operations. This Phase I project experimentally studied various drill geometry and process parameters believed to contribute to burr formation. Analysis of the data indicated drill point angle, type of clamp and distance from the hole to the camp as being the most significant factors in causing interfacial burrs. Further, drill feed per revolution, spindle speed (RPM) and point type, including specially ground step drills, also displayed a significant impact on interfacial burr formation. Comparisons of alternate drill geometries to the drill currently used by Lockheed-Martin indicate potential changes which may serve to significantly reduce interfacial burr formation.

Introduction

Burr formation is common to nearly all machining operations. In drilling a through-hole, both an entry and exit burr will form. Consequently, in the drilling of a through-hole in two stacked sheets, burrs will form at the interface of the two sheets, as shown in Figure 1. Minimizing or eliminating these burrs may prevent the need for de-stacking and deburring operations. Drilling of stacked sheets is a frequent operation in aircraft structure assembly in general, and specifically at Lockheed Martin. This project studied interfacial burr formation in an attempt to find the major contributing factors and develop a strategy to minimize or eliminate interfacial burrs. It is believed that minimization of interfacial burr will also tend to minimize any initial entry and final exit burrs.

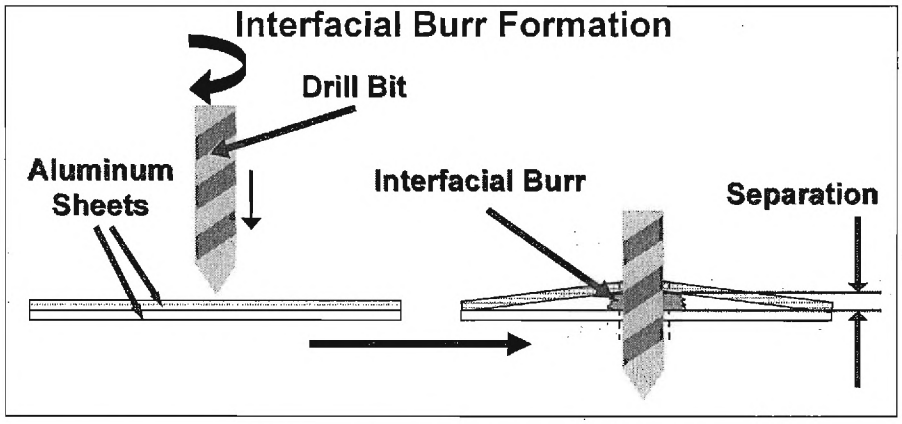

Figure 1. Interfacial burr formation in drilling of two stacked sheets

Experimental Set-up

In order to identify the major factors responsible for burr formation, a literature survey was conducted. Little existing work detailing the drilling of stacked sheets has been reported. Consequently, factors which have been shown as significant to burr formation in general have been selected. The factors and their levels can be seen in Table 1. Helix angle, point angle, coating type and point type comprise the various elements of drill geometry examined. These parameters are often altered for different applications, meaning numerous combinations are readily available. All drills were #10 in size (0.1935"diameter). Note that while drill wear will impact burr formation, for simplicity, it was not considered as a factor in this experiment. Each run of the experiment was conducted with a new drill to remove the effect of drill wear.

Table 1. Experimental factors and their levels

Factor	Level 0	Level 1	Level 2
Helix Angle	20° (standard)	30° (high)	-
Point Angle	118° (standard)	135°	-
Coating	Black Oxide	TiN	-
Point Type	Standard	Split	Step (mixed standard and split)
Feed	0.004 in/rev	0.0065 in/rev	0.009 in/rev
Speed	3000 RPM	4500 RPM	6000 RPM
Clamp Type	2 Clamps	1 Clamp	1 Clamp, 1 Cleco
Clamp Distance	15 mm (0.59")	35 mm (1.38")	55 mm (2.17")
Frame Material	2024T3	7070T6	-

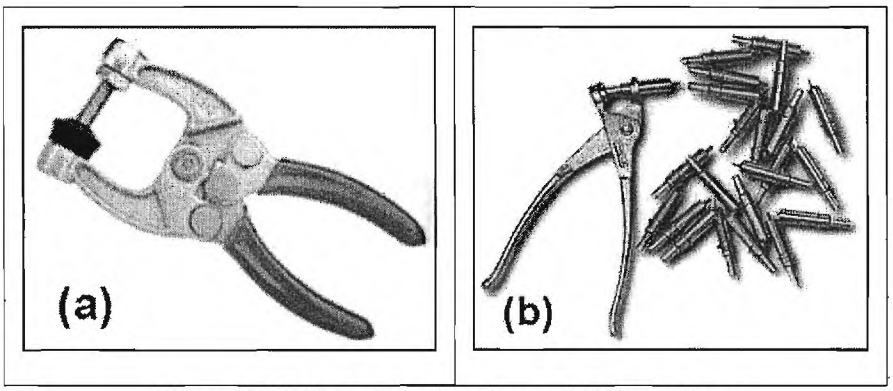

Figure 2. (a) Squeeze-action clamp, (b) Cleco clamp

The feeds and speeds selected were based on current Lockheed Martin practices and reported research in drilling of aluminum (Huang and Lin, 2004; Rivero et. al, 2005). The clamps used were De-Sta-Co model 424 squeeze action clamps, shown in Figure 2(a). This type of clamp is rated at 200 lbs. The Cleco clamp, see Figure 2(b), is a plier-operated spring-loaded hole clamp. This type of clamp

is frequently used in sheet-metal assembly, and is used extensively by Lockheed. It serves to align pre-existing holes in sheets and to provide moderate clamping force. The sheet materials were 2024-T351 and 7075-T651 aluminum alloy, both extremely common in aircraft structures. The top sheet, called the skin, was always 2024, while the bottom sheet, known as the frame, was either material. Aluminum 2024 was always used for the skin since it is more ductile than 7075 and will presumably be the "worst-case" skin material in terms of burr formation.The drill point type factor was divided into three levels. The cases of a standard-point, split-point and step drill were considered. The step drill utilized, displayed below in Figure 3, was chosen based on results from the literature (Ko et. al., 2003).

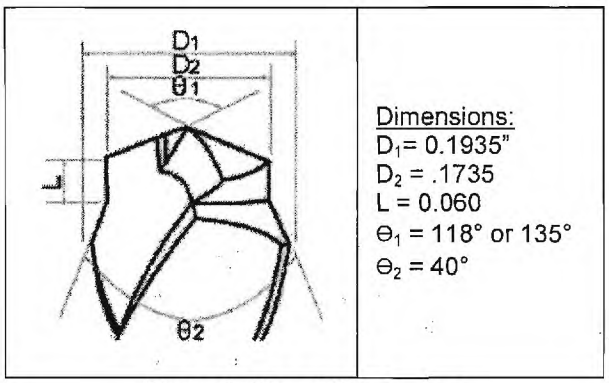

Figure 3. Step drill geometry

The actual experimental setup is shown in Figure 4(a). It can be seen that a clamp has been placed to the left of the drilled hole and a Cleco has been placed to the right, and in line with the clamp and hole. The lower sheet, or frame, was a section of 90° angle screwed to a fixture. Both the skin and the frame were 1/16" in thickness. The three clamping arrangements are given in Figure 4(b). Note that a clamp was always placed to the left of the drilled hole, and the "distance from clamp" factor was always measured relative to the center of this clamp. Hence, in the third case shown, the hole is drilled 15 mm (0.59") from the left clamp, but is also 55 mm (2.17") from the Cleco located on the right.

In an effort to balance the large number of factors to be analyzed with the available time and money while maximizing the knowledge gained from the tests, a 36-run restricted partially-orthogonal array was designed, and can be found in Appendix A. Two replicates of the experimental design were conducted for a total of 72 runs. The design was restricted in the sense that the drill geometry related factors were not completely balanced. This was due to the selection of drill geometries which are readily available. The step drills were created by custom-grinding the step geometry into drills which were purchased off-the-shelf. It was also determined that certain combinations of the geometry factors are not

available since they cannot physically be ground on the drill. The drills utilized in this project are given below in Table 2. Note that drill 5 is currently used by Lockheed Martin.

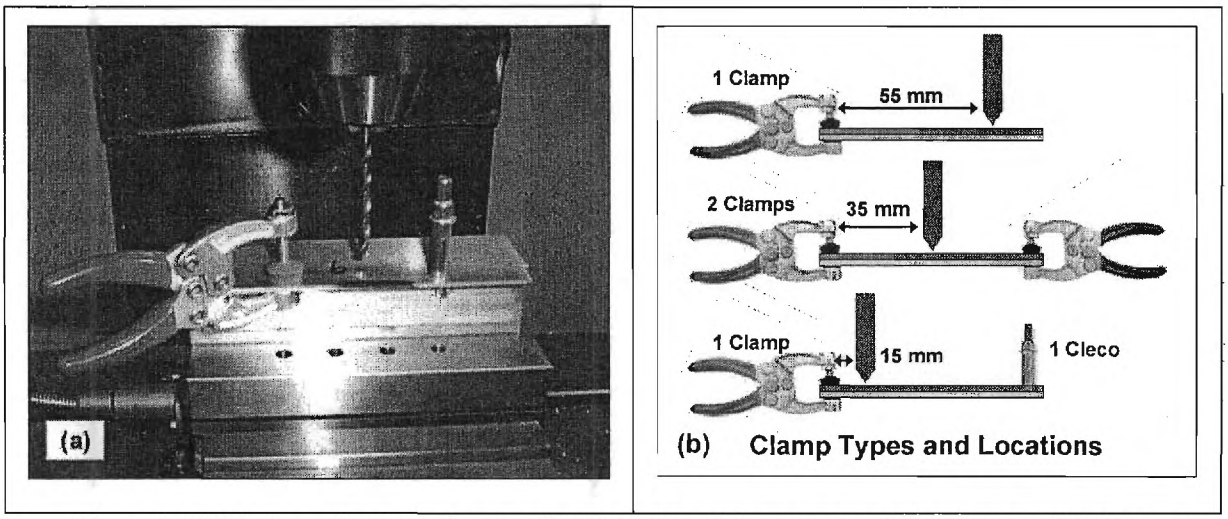

Figure 4. (a) Photograph of sample setup (b) Examples of clamp type and location combinations

Table 2. Descriptions of each drill bit used in the experiment

Drill	Helix	Point Angle	Coating	Point Type
1	20°	118°	Black oxide	Standard, no step
2	20°	118°	Black oxide	Split, no step
3	20°	118°	Black oxide	Split, Step
4	20°	118°	TiN	Standard, no step
5	20°	135°	Black oxide	Split, no step
6	20°	135°	TiN	Split, no step
7	20°	135°	Black oxide	Split, Step
8	30°	118°	Uncoated	Standard, no step
9	30°	118°	Uncoated	Standard, step

Measurements

Burrs are small, uneven and easily deformable, making measurement of burrs inherently difficult. For these experiments, three methods of interfacial burr measurement were employed. The first method was to measure the post-drilling separation of the two sheets. While not a direct measurement of the burr height, it is nonetheless correlated with it. Using this method, a micrometer reading was taken of the total sheet thickness near the hole before and after the drilling operation, while the sheets were still clamped. Comparison of the two measurements yielded the post-drilling separation. In the second interfacial burr measurement technique, a video was taken of each drilling operation. From the videos, the instantaneous sheet separation could be monitored. Additionally, this method provided a record of chip entrapment, cap burrs, and any other unusual phenomena that occurred during the test. The last burr measurement technique was to study each sheet individually on an optical comparator. By placing a gage block near the burr and bringing both into focus, the difference from the maximum point of the burr to the top of the gage block could be accurately recorded. Knowing the thickness of the gage block, the maximum burr height could be found. Utilizing this method, both the skin exit burr and the frame entry burr could be measured individually. Each burr was measured from 4 different orientations. The skin entry and frame exit burrs were not examined.

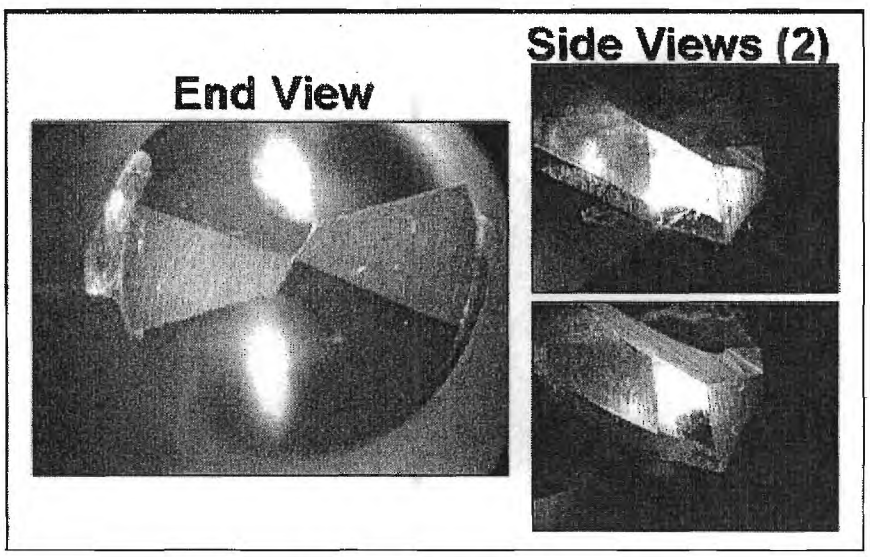

Figure 5. Sample drill characterizations

Though all three measurement methods were used in each experiment, it was determined that the optical comparator measurements would be used as the primary source of burr height data. The post-drilling separation micrometer readings and the optical comparator readings both offered an appropriate

level of accuracy, but the optical comparator method was superior for two reasons. First, it allowed for individual measurements of both the skin exit and frame entry burrs. Second, the interfacial burrs of the de-stacked sheets most closely matched what a worker would see when deburring drilled holes during the manufacturing process, thus it was the most pertinent measurement.

In addition to burr measurements, each drill was characterized with a toolmaker's microscope both before and after the drilling operation. Sample images of a step drill are displayed above in Figure 5. Images of each burr were also taken to monitor its nature. A 3-axis Kistler piezoelectric force dynamometer was utilized in each test to capture the drilling thrust force. A sample plot of the thrust forces is given in Figure 6. This graph is typical of what was observed across all the tests. Note that drilling torque was not monitored during testing.

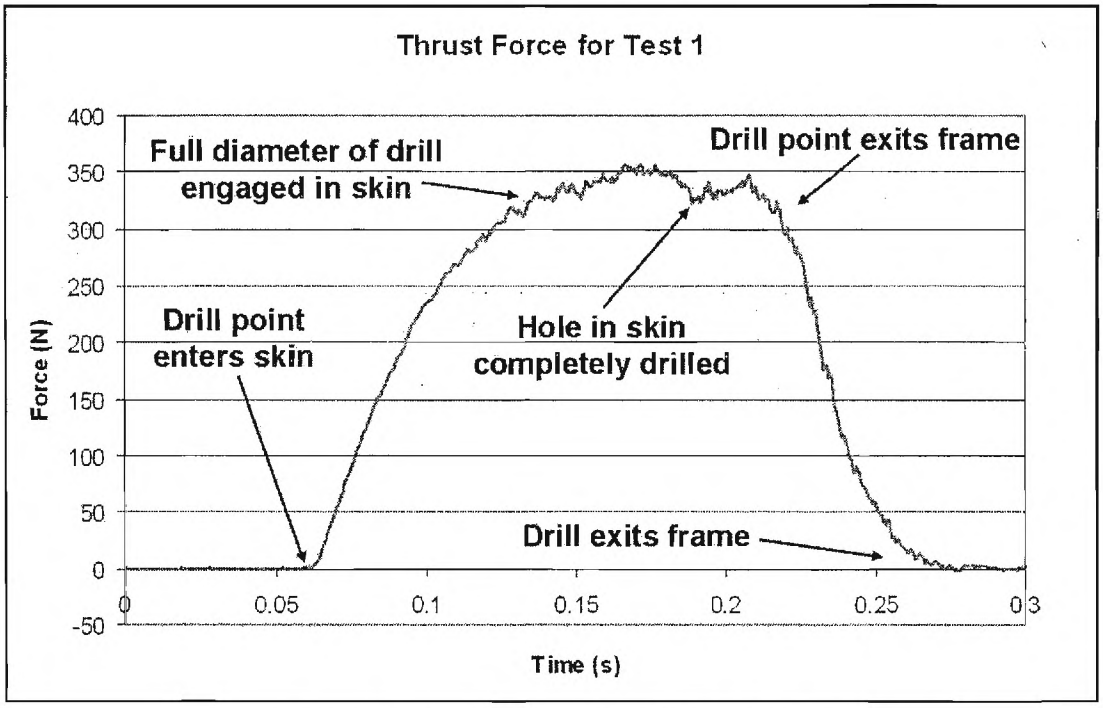

Figure 6. Sample drilling thrust force profile

Results

Still frames from the videos of two example cases are shown below. Figure 7(a) and (b) are from runs 23 and 26 of the first replicate, respectively. The complete details of the parameters used in each test are given in Table A.2 of Appendix A. Figure 7(a) shows drill 5, the current Lockheed Martin drill, in a case where only a single clamp was located to the left. Notice the initial separation of the two sheets, which was closed by the force of the drill. Once the hole in the skin was completely drilled, the skin sheet sprung up and allowed chips to become entrapped in the interface. Lastly, a cap burr is evident at the frame exit burr. Figure 7(b) shows the case of drill 3, the same drill as the Lockheed Martin drill, but with a 118° point angle and a step. This hole was located near a Cleco. Minimal separation is shown, and no cap burr is formed at the frame exit burr.

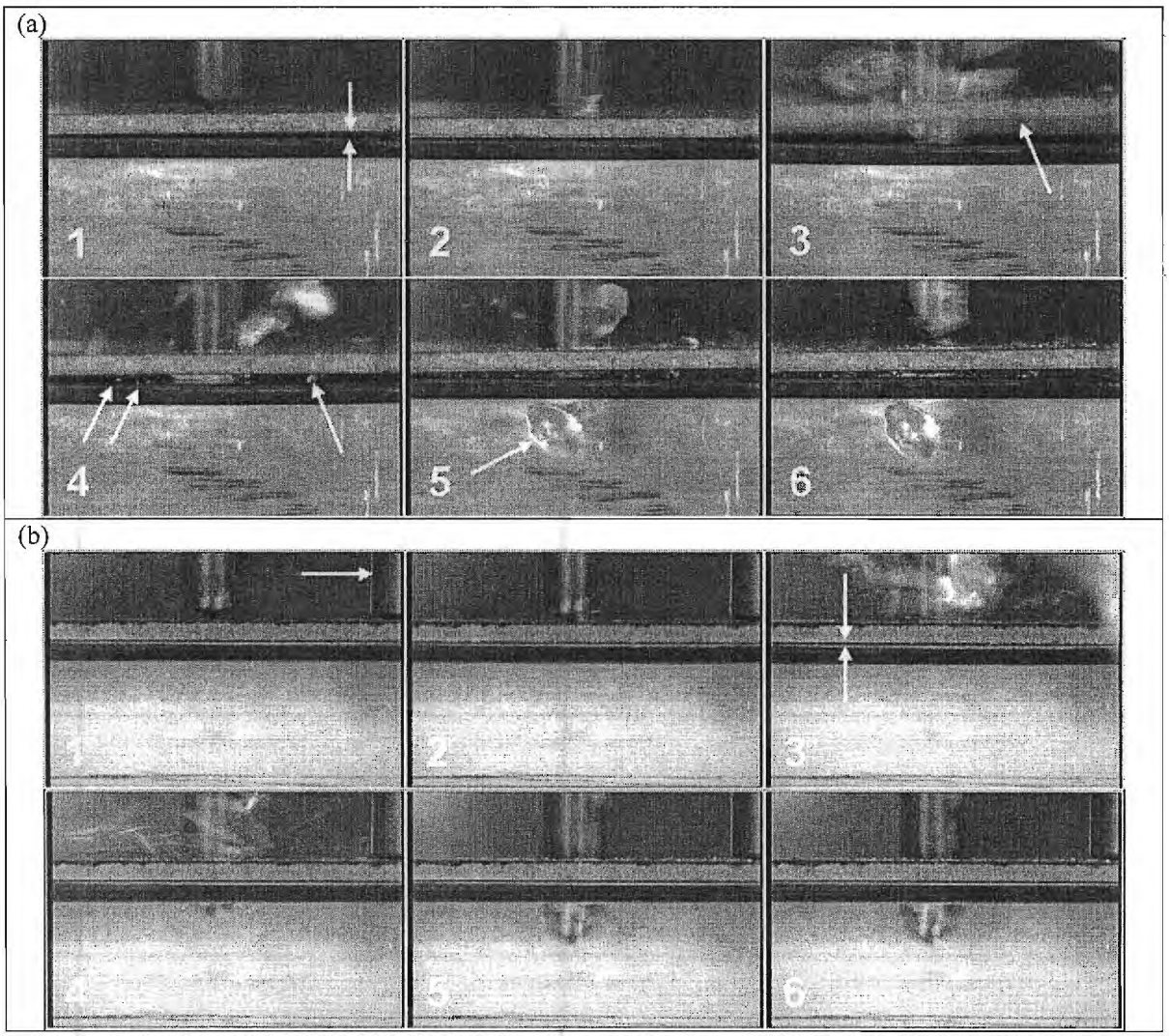

Figure 7. (a) Current LMCO drill (Drill 5) in with a single clamp (b) Drill 3 with 1 clamp and 1 Cleco

The raw data gathered can be seen in Appendix B. For all of the analysis of the optical comparator readings, the average of the largest three maximum burr height measurements (out of four) was taken as a single data point for each interfacial burr. Figure 8 shows the main effects of the optical comparator measurements of the skin exit burr and frame entry burr. Notice that the skin exit burr had an average of 0.0035" and the frame entry burr had an average of 0.0030". Similar trends for both burr types were apparent. The skin exit burr was the greater of the two burrs in nearly every case.

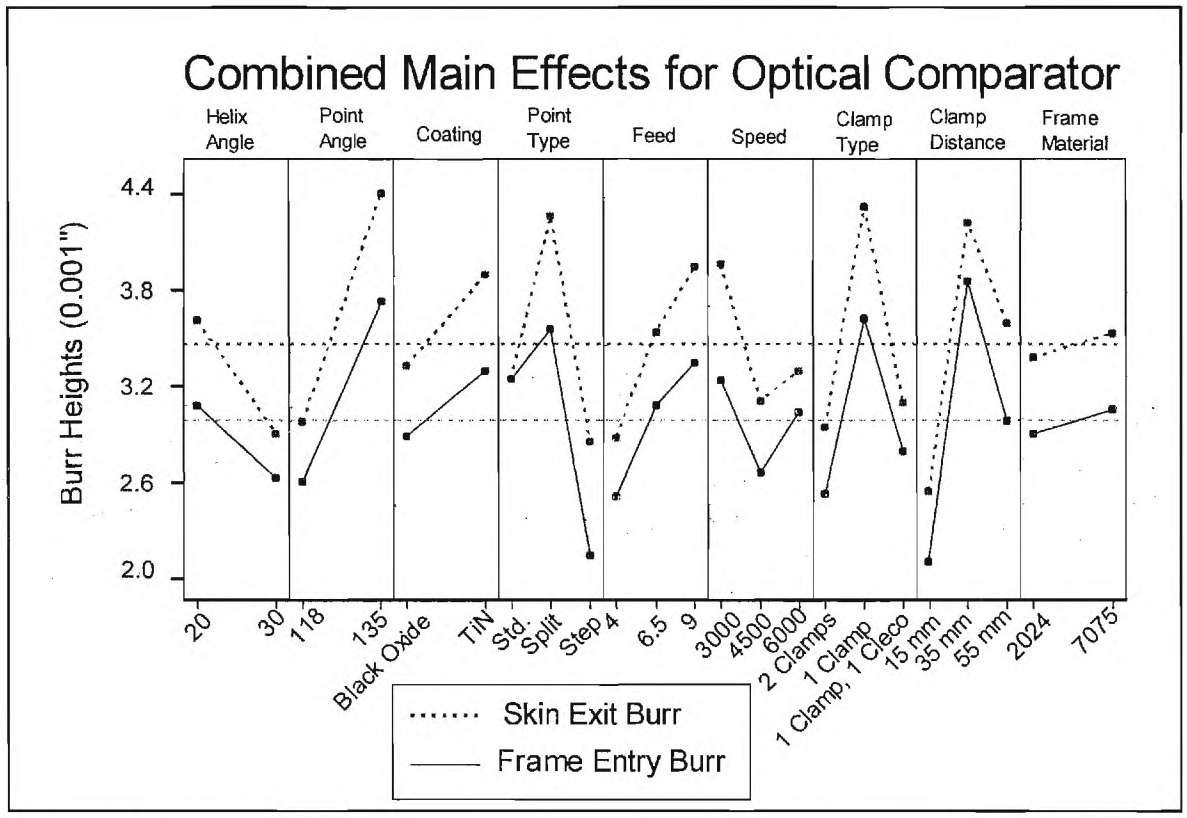

Figure 8. Main effects plot for optical comparator readings of skin exit burr and frame entry burr

To determine which of the observed trends are significant, statistical analysis must be performed. ANOVA tables can be found in Appendix C. Effects were considered significant with an alpha value of 0.1, though most effects had considerably smaller p-values. The significant main effects for the skin exit burr measurements are given in Figure 9. Note that the 118° point angle outperformed the 135° point angle. The maximum average burr height increased with increasing feed, which is consistent with data in the literature.

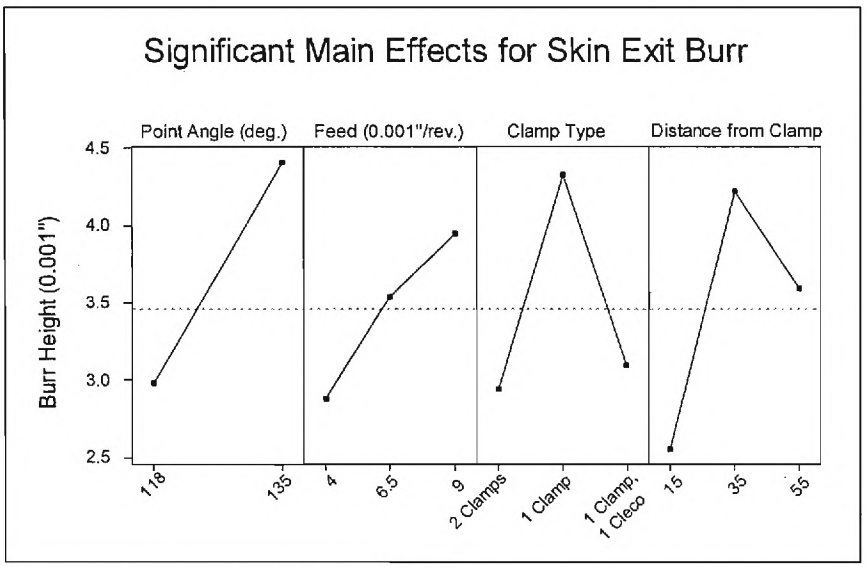

Figure 9. Significant main effects for skin exit burr optical comparator measurements

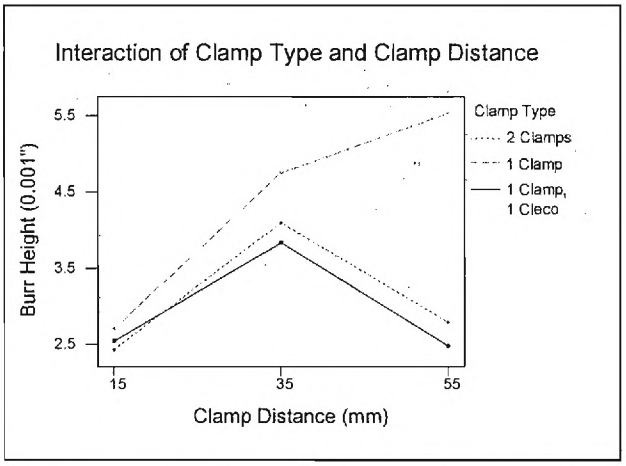

Figure 10. Interaction of clamp type and clamp distance on the skin exit burr optical comparator measurements

Due to the nature of the clamp type and distance from clamp factors, it is beneficial to observe the interaction of the two, seen above in Figure 10. Notice that both cases of two supports exhibited a similar trend. In both, the burr was smallest near a clamp or Cleco, and largest in the center. In the arrangement of a single clamp, the burr height increases with the distance of the hole away from the clamp. These trends can be explained by the fact that the stacked sheets act as either a simply supported or a cantilevered beam that deflects elastically under the drilling thrust force. The deflection is maximum in the center, thus causing greater separation between the two sheets. In the case of a single clamp

(cantilevered beam arrangement), the deflection (and separation) is greatest further away from the clamped end. Consequently, the burr height increases with clamp distance.

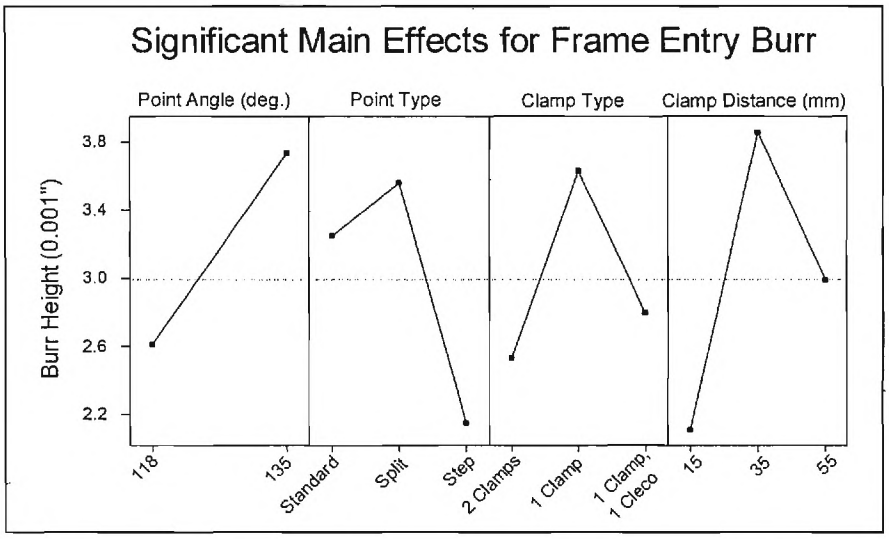

Figure 11. Significant main effects for frame entry burr optical comparator measurements

Performing the same analysis on the frame entry burr optical comparator measurements yielded the effects found in Figure 11. Point angle, clamp type and clamp distance were again found to be significant. In place of feed, the point type was now found to be a significant factor. It is shown that while a standard point outperformed a split point, a step drill outperformed either non-step drill.

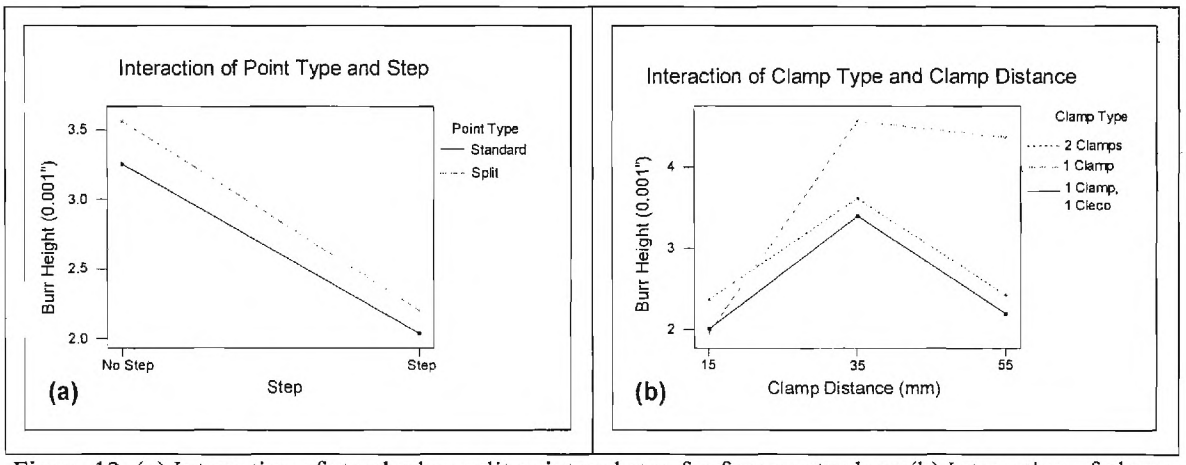

Figure 12. (a) Interaction of standard or split point and step for frame entry burr (b) Interaction of clamp type and clamp distance from frame entry burr

Observing the interaction of split and standard points with a step, as in Figure 12(a), it is clear that the effect of the step was far more pronounced than the effect of the standard or split point. Figure 12(b) gives the interaction of clamp type and clamp distance effects, which was similar to the case of the skin exit burr.

Turning now to the post-drilling separation micrometer readings, the same trends that were seen in the optical comparator readings are found. The average value of post-drilling separation, across all tests, was approximately 0.0020". This was smaller than either the individual skin exit or frame entry burrs observed above. This was likely due to the fact that the micrometer measurements were taken while the part was still clamped. When interfacial burrs are formed, the skin exit burr and the frame entry burr become entangled and intertwined. Upon de-stacking the sheets, the burrs are untangled and deformed.

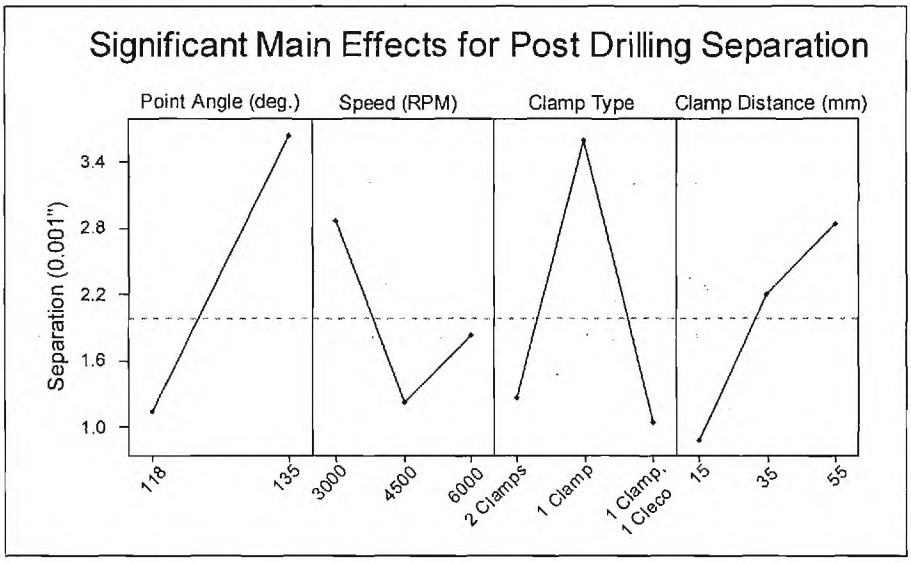

Figure 13. Significant main effects of post-drilling separation micrometer measurements

The statistically significant main effects for post-drilling separation are shown above in Figure 13. The statistical analysis indicated that speed was only possibly significant, though it has been included here for completeness. Point angle, clamp type and clamp distance were again significant effects, as they were for both individual burr measurement cases. This indicates that these three factors are perhaps the most significant, more so than feed, point type or speed, which only appear once – either in the individual burr measurement analysis or in the post-drilling separation analysis. Figure 14 demonstrates the clamp type and distance from clamp interaction. As expected, the case of a single clamp located at the largest distance generated the largest maximum burr height for any clamping arrangement.

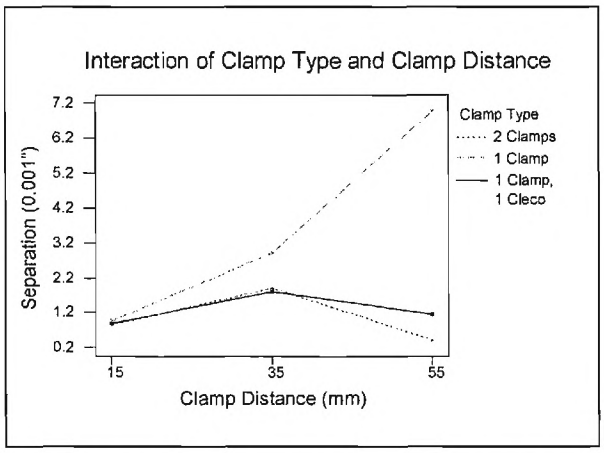

Figure 14. Interaction of clamp type and clamp distance for post-drilling separation micrometer measurements

To analyze the data in a different manner, the results have been plotted against each combination of drill geometry tested, and can be seen in Figure 15. The drill geometries are given above in Table 2 of the experimental set-up section. The error bars in Figure 15 denote a single standard deviation of the data. The graph seems to indicate that drill 5, the current Lockheed Martin drill, generated the largest burr of any case, with a large variance in the data. As predicted by the point angle trends, switching from the drill 5 to drill 2, an identical drill except with a 118° point, served to decrease the maximum burr height. Drill 3 adds a step to drill 2, and further reduced burr height to its lowest value, with a low variance.

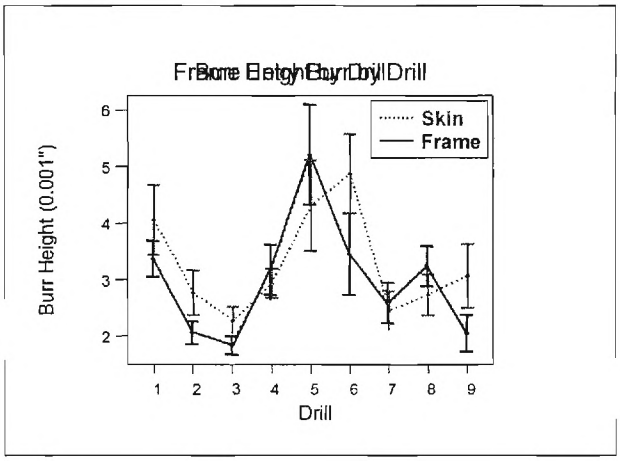

Figure 15. Skin exit and frame entry burr heights by drill (error bars denote 1 standard deviation)

However, it is important to recognize that due to the limited number of runs in the experimental design, each drill was only tested at 4 combinations of the 5 factors unrelated to drill geometry. In fact, no drill was tested at the exact same conditions as any other drill. For this reason, more weight should be given to the individual drill geometry aspect trends seen previously in Figure 8 than to the trends in Figure 15. With that in mind, it is still fair to say that drills 2 and 3 tend to produce a smaller burr than drill 5, the drill currently used by Lockheed Martin.

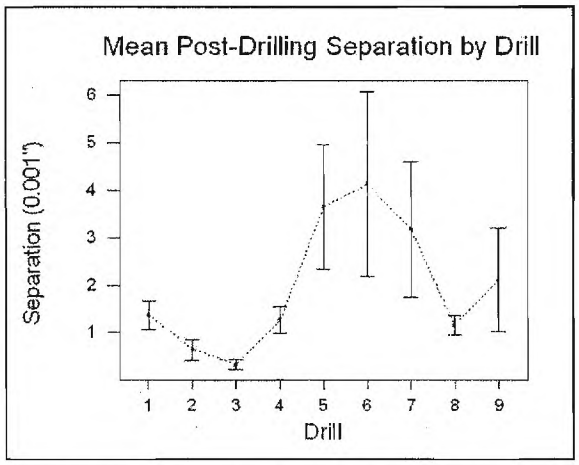

Figure 16. Post-drilling separation by drill (error bars denote 1 standard deviation)

Creating a similar plot of post-drilling separation by drill, Figure 16, a similar trend is found. As before, the current Lockheed Martin drill, drill 5, demonstrated relatively poor performance and large variability. Drill 2 performed better than drill 5, and drill 3 outperformed all drills. Both drills 2 and 3 had small variability in their data. The same caution should be taken in drawing conclusions from Figure 16 as from Figure 15.

The drilling thrust force data was examined, and the instantaneous force when the drill point broke through the skin was determined and used for analysis. The statistically significant main effects have been plotted in Figure 17. The two components of drill geometry which impacted thrust force are helix angle and coating type. Point type, feed and speed had a significant effect on thrust force, as well as on interfacial burr formation which indicates a possible correlation. Interfacial burr heights followed the same trends as thrust force for the effects of feed and speed. Step drills reduced thrust force as well as burr height. Conversely, though standard points demonstrated a lower burr height than split points, they required a much greater thrust force.

From studying the videos, chip entrapment in the interface could be monitored. It was found that chip entrapment occurred only in cases of a single clamp 35 mm (1.38") or greater away. It is also worth noting that in most cases, chip entrapment occurred in only one of the two replicates conducted.

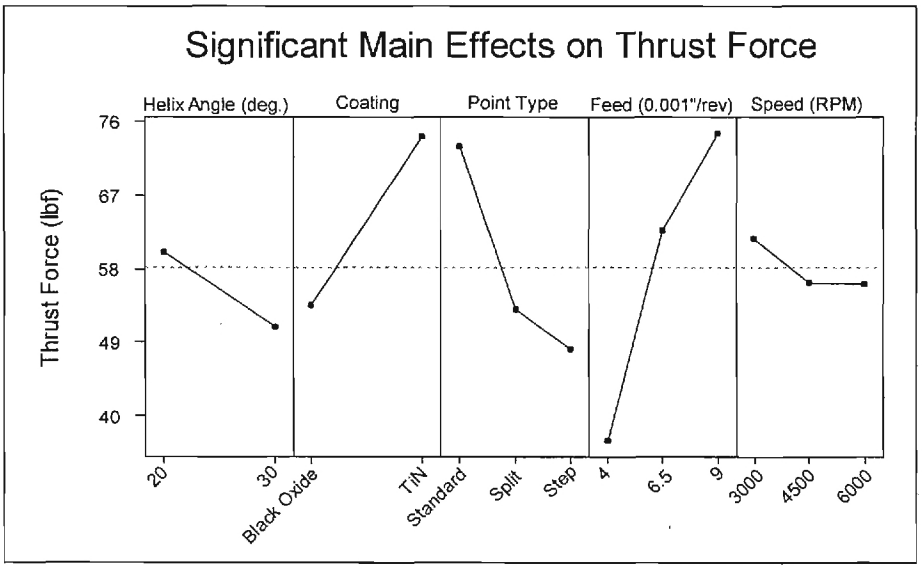

Figure 17. Significant main effects on thrust force

Conclusions

It was found through optical comparator measurements that interfacial skin exit burrs and frame entry burrs demonstrated a similar dependence upon all the examined parameters. Averaged across all tests, frame entry burrs were approximately 15% smaller than skin exit burrs. It was found that the most significant factors in interfacial burr formation were drill point angle, clamp type and clamping distance. A combination of a 118° point angle with a hole location near a clamp or Cleco reduced the interfacial burr heights. Additionally, the analysis revealed that smaller feeds produced smaller skin exit burrs, while the use of a step drill reduced the frame entry burr. It is believed that these trends will hold true for both types of interfacial burrs.

The post-drilling separation micrometer readings demonstrated similar trends to the optical comparator maximum burr height measurements, though with a lower magnitude. It was also found the feed per revolution had the most dramatic impact on the drilling thrust forces. Though standard point drills slightly outperformed split point drills in terms of burr height, split points required a much lower drilling thrust force. Lastly, it was found that chip entrapment in the interface occurred only in cases of a single clamp 35 mm (1.38") or greater from the hole location.

Taking into account the findings of this report, the authors make the following recommendations to minimize interfacial burrs:

- Drill point angle should be 118°
- Holes should be located near a clamp or Cleco
- If only a single support is present, holes should be less than a distance of 35 mm (1.38") away from the support to prevent chip entrapment
- Drill should have a split-point
- Step drill should be considered, where cost effective
- Feed should be limited

References

Huang, M.-F., Lin, T.-R., "Application of grey-Taguchi method to optimize drilling of aluminum alloy 6061 with multiple performance characteristics," Materials Science and Technology, Vol. 20, pp. 528-532, 2004.

Ko, S.-L., Chang, J.-E., Yang, G.-E., "Burr Minimization Scheme in Drilling," Journal of Materials Processing Technology, Vol. 140, No. 1-3, pp. 237-242, 2003.

Rivero A., Aramendi, G., Herranz, S., López de Lacalle, L.N., "An Experimental investigation of the effect of coatings and cutting parameters on the dry drilling performance of Aluminum alloys," International Journal of Advanced Manufacturing Technology, Vol. 28, pp. 1-11, 2006.

APPENDIX A: Design of Experiment

Table A.1. 36-Run restricted partially orthogonal array (coded)

Factor	Description	Level 0	Level 1	Level 2
A	helix angle	20	30	-
B	point angle	118	135	-
C	coating	None	TiN	-
D	point type	Standard	Split	Step
E	feed	0.004 in/rev	0.0065 in/rev	0.009 in/rev
F	speed	3000 RPM	4500 RPM	6000 RPM
G	clamp type	2 clamps	1 clamp	1 clamp, 1 cleco
H	dist from clamp	15 mm	35 mm	55 mm
I	frame type	2024	7070	-

Run #	A	B	C	D	E	F	G	H	I
1	0	1	1	1	1	2	0	1	1
2	0	0	0	1	0	0	2	2	1
3	0	1	0	2	2	1	1	0	0
4	0	0	0	1	0	0	0	0	1
5	0	0	0	2	1	2	1	0	1
6	0	0	0	2	2	1	2	2	1
7	0	0	0	0	2	2	0	2	0
8	0	1	0	1	0	0	2	1	0
9	1	0	0	0	2	1	0	1	0
10	0	1	0	2	1	2	2	0	1
11	0	1	0	1	1	0	1	2	0
12	0	0	0	1	0	1	1	1	0
13	0	1	1	1	2	0	1	2	1
14	0	0	0	0	1	1	0	0	1
15	0	0	1	0	0	2	2	1	0
16	1	0	0	0	1	1	1	1	1
17	0	0	0	0	2	0	2	1	1
18	0	0	0	1	0	2	0	0	1
19	1	0	0	2	0	0	1	0	0
20	0	1	1	1	1	1	0	2	0
21	0	1	0	2	0	2	1	2	0
22	0	0	1	0	2	0	0	1	1
23	1	0	0	0	2	1	2	0	0
24	0	0	1	0	1	2	2	2	0
25	0	1	1	1	0	1	2	0	1
26	0	1	0	1	2	2	1	1	1
27	0	0	0	2	1	0	0	2	0
28	0	0	0	2	2	2	2	2	1
29	1	0	0	2	0	1	0	2	1
30	1	0	0	2	1	0	1	1	1
31	0	0	0	0	1	1	2	1	0
32	1	0	0	2	2	2	1	0	0
33	0	0	1	0	1	0	2	0	0

34	1	0	0	0	0	1	1	2	1
35	0	1	0	2	0	2	0	1	0
36	0	1	0	1	2	0	0	0	0

Factor Correlations:

	A	B	C	D	E	F	G	H	I
A	1								
B	-0.377	1							
C	-0.285	0.188	1						
D	0	0.288	-0.327	1					
E	0	0	0	-0.125	1				
F	-0.081	0.072	0	0.125	0	1			
G	-0.081	-0.072	0.081	-0.083	0	0	1		
H	-0.081	0	0.081	0	0	0	0	1	
I	0	-0.117	0	0.068	0	0	0	0	1

Table A.2. Randomized design of first replicate

Run #	Drill #	Speed (RPM)	Feed Rate (ipm)	Clamp	Dist	Frame	Orig. Run #
1	9	3000	12	1-Vise	15 mm	2024	19
2	2	6000	24	2-Vise	15 mm	7075	18
3	4	3000	19.5	1-Vise, 1-Cleco	15 mm	2024	33
4	6	4500	18	1-Vise, 1-Cleco	15 mm	7075	25
5	9	3000	19.5	1-Vise	35 mm	7075	30
6	6	4500	29.25	2-Vise	55 mm	2024	20
7	7	6000	39	1-Vise, 1-Cleco	15 mm	7075	10
8	9	4500	18	2-Vise	55 mm	7075	29
9	1	3000	27	1-Vise, 1-Cleco	35 mm	7075	17
10	3	6000	54	1-Vise, 1-Cleco	55 mm	7075	28
11	1	4500	29.25	2-Vise	15 mm	7075	14
12	9	6000	54	1-Vise	15 mm	2024	32
13	2	3000	12	1-Vise, 1-Cleco	55 mm	7075	2
14	2	3000	12	2-Vise	15 mm	7075	4
15	6	3000	27	1-Vise	55 mm	7075	13
16	5	6000	54	1-Vise	35 mm	7075	26
17	5	3000	12	1-Vise, 1-Cleco	35 mm	2024	8
18	8	4500	40.5	1-Vise, 1-Cleco	15 mm	2024	23
19	5	3000	27	2-Vise	15 mm	2024	36
20*	3	3000	19.5	2-Vise	55 mm	2024	27
21	8	4500	18	1-Vise	55 mm	7075	34
22	4	3000	27	2-Vise	35 mm	7075	22
23	5	3000	19.5	1-Vise	55 mm	2024	11
24*	6	6000	39	2-Vise	35 mm	7075	1
25	2	4500	18	1-Vise	35 mm	2024	12
26	3	4500	40.5	1-Vise, 1-Cleco	55 mm	7075	6
27	7	6000	24	1-Vise	55 mm	2024	21
28	4	6000	39	1-Vise, 1-Cleco	55 mm	2024	24
29	8	4500	29.25	1-Vise	35 mm	7075	16
30	1	4500	29.25	1-Vise, 1-Cleco	35 mm	2024	31
31	3	6000	39	1-Vise	15 mm	7075	5
32	7	4500	40.5	1-Vise	15 mm	2024	3
33	7	6000	24	2-Vise	35 mm	2024	35
34	1	6000	54	2-Vise	55 mm	2024	7
35	8	4500	40.5	2-Vise	35 mm	2024	9
36	4	6000	24	1-Vise, 1-Cleco	35 mm	2024	15

* Denotes a botched experiment which was repeated in Replicate 3 (Table A.4)

Table A.3. Randomized design of second replicate

Run #	Drill #	Speed (RPM)	Feed Rate (ipm)	Clamp	Dist	Frame	Orig. Run #
1	5	6000	54	1-Vise	35 mm	7075	26
2	1	4500	29.25	1-Vise, 1-Cleco	35 mm	2024	31
3	2	6000	24	2-Vise	15 mm	7075	18
4	8	4500	29.25	1-Vise	35 mm	7075	16
5	6	3000	27	1-Vise	55 mm	7075	13
6	4	3000	19.5	1-Vise, 1-Cleco	15 mm	2024	33
7	8	4500	40.5	2-Vise	35 mm	2024	9
8	3	6000	54	1-Vise, 1-Cleco	55 mm	7075	28
9	5	3000	12	1-Vise, 1-Cleco	35 mm	2024	8
10	2	3000	12	1-Vise, 1-Cleco	55 mm	7075	2
11	1	3000	27	1-Vise, 1-Cleco	35 mm	7075	17
12	8	4500	40.5	1-Vise, 1-Cleco	15 mm	2024	23
13	6	6000	39	2-Vise	35 mm	7075	1
14	1	6000	54	2-Vise	55 mm	2024	7
15	7	6000	24	1-Vise	55 mm	2024	21
16	9	4500	18	2-Vise	55 mm	7075	29
17	9	6000	54	1-Vise	15 mm	2024	32
18	3	3000	19.5	2-Vise	55 mm	2024	27
19	9	3000	12	1-Vise	15 mm	2024	19
20	3	4500	40.5	1-Vise, 1-Cleco	55 mm	7075	6
21	2	4500	18	1-Vise	35 mm	2024	12
22	6	4500	29.25	2-Vise	55 mm	2024	20
23	8	4500	18	1-Vise	55 mm	7075	34
24	7	6000	24	2-Vise	35 mm	2024	35
25	4	3000	27	2-Vise	35 mm	7075	22
26	7	6000	39	1-Vise, 1-Cleco	15 mm	7075	10
27	1	4500	29.25	2-Vise	15 mm	7075	14
28	9	3000	19.5	1-Vise	35 mm	7075	30
29	5	3000	19.5	1-Vise	55 mm	2024	11
30*	4	6000	39	1-Vise, 1-Cleco	55 mm	2024	24
31	2	3000	12	2-Vise	15 mm	7075	4
32	6	4500	18	1-Vise, 1-Cleco	15 mm	7075	25
33	5	3000	27	2-Vise	15 mm	2024	36
34	3	6000	39	1-Vise	15 mm	7075	5
35	4	6000	24	1-Vise, 1-Cleco	35 mm	2024	15
36	7	4500	40.5	1-Vise	15 mm	2024	3

* Denotes a botched experiment which was repeated in Replicate 3 (Table A.4)

Table A.4. Randomized design of third replicate to make up botched runs

Run #	Drill #	Speed (RPM)	Feed Rate (ipm)	Clamp	Dist	Frame	Orig. Run #
1	4	6000	39	1-Vise, 1-Cleco	55 mm	2027	24
2	3	3000	19.5	2-Vise	55 mm	2024	27
3	6	6000	39	2-Vise	35 mm	7075	1

APPENDIX B: Results

Table B.1. Maximum skin exit burr measurements for first replicate (in experimental order)

Run	Skin (0.001") (4 orientations)				Mean	Max	Avg. Top 3
1	3.0	4.8	4.9	2.4	3.78	4.9	4.2
2	1.2	1.9	1.9	1.6	1.65	1.9	1.8
3	2.3	2.3	2.7	1.6	2.23	2.7	2.4
4	2.3	2.9	3.2	2.9	2.83	3.2	3.0
5	5.2	5.6	6.6	4.5	5.48	6.6	5.8
6	2.8	4.6	3.5	3.6	3.63	4.6	3.9
7	0.6	1.8	1.2	1.6	1.30	1.8	1.5
8	1.1	2.6	1.9	1.2	1.70	2.6	1.9
9	5.8	6.7	6.2	5.1	5.95	6.7	6.2
10	1.2	3.0	1.8	2.3	2.08	3.0	2.4
11	2.3	2.5	3.4	1.1	2.33	3.4	2.7
12	1.3	2.3	1.7	0.0	1.33	2.3	1.8
13	2.3	3.9	3.1	3.3	3.15	3.9	3.4
14	1.9	2.5	2.4	2.3	2.28	2.5	2.4
15	6.2	6.9	6.7	6.9	6.68	6.9	6.8
16	6.0	6.2	5.6	5.0	5.70	6.2	5.9
17	3.2	4.3	4.3	4.1	3.98	4.3	4.2
18	1.9	2.7	3.4	1.8	2.45	3.4	2.7
19	2.0	2.9	2.8	1.8	2.38	2.9	2.6
20*	1.0	1.9	1.4	2.2	1.63	2.2	1.8
21	1.4	1.4	1.3	1.8	1.48	1.8	1.5
22	3.3	4.2	3.8	4.5	3.95	4.5	4.2
23	10.4	11.7	11.0	11.3	11.10	11.7	11.3
24*	4.4	5.9	5.1	5.5	5.23	5.9	5.5
25	4.2	5.1	4.4	3.9	4.40	5.1	4.6
26	2.3	2.6	3.7	1.7	2.58	3.7	2.9
27	7.4	8.9	8.8	7.6	8.18	8.9	8.4
28	1.9	2.4	3.1	2.3	2.43	3.1	2.6
29	2.4	2.6	2.5	1.5	2.25	2.6	2.5
30	2.4	3.8	3.7	3.0	3.23	3.8	3.5
31	1.3	2.1	1.6	2.0	1.75	2.1	1.9
32	1.9	2.2	2.4	2.7	2.30	2.7	2.4
33	1.3	2.6	2.7	1.7	2.08	2.7	2.3
34	1.3	2.6	2.7	1.7	2.08	2.7	2.3
35	1.5	2.3	2.6	2.6	2.25	2.6	2.5
36	1.4	3.2	3.0	2.1	2.43	3.2	2.8

*Appropriate values from third replicate substituted for botched tests

Table B.3. Maximum frame entry burr measurements for first replicate (in experimental order)

Run	Frame (0.001") (4 orientations)				Mean	Max	Avg. Top 3
1	0.8	1.5	0.8	0.6	0.93	1.5	1.0
2	1.6	1.5	0.5	1.7	1.33	1.7	1.6
3	5.8	5.8	6.1	6.0	5.93	6.1	6.0
4	1.3	0.5	1.1	1.4	1.08	1.4	1.3
5	2.0	2.1	1.7	1.1	1.73	2.1	1.9
6	1.3	0.8	2.3	2.6	1.75	2.6	2.1
7	0.9	1.0	0.9	1.0	0.95	1.0	1.0
8	1.5	0.6	0.9	0.4	0.85	1.5	1.0
9	4.2	3.6	6.0	4.1	4.48	6.0	4.8
10	2.3	2.4	2.3	1.7	2.18	2.4	2.3
11	1.9	1.9	2.1	2.2	2.03	2.2	2.1
12	0.6	1.9	1.2	1.9	1.40	1.9	1.7
13	2.1	1.7	3.4	2.0	2.30	3.4	2.5
14	1.4	1.7	0.7	3.0	1.70	3.0	2.0
15	5.5	4.4	5.0	5.2	5.03	5.5	5.2
16	8.9	9.3	9.0	9.1	9.08	9.3	9.1
17	4.5	4.5	1.8	3.8	3.65	4.5	4.3
18	1.3	1.4	1.8	1.6	1.53	1.8	1.6
19	0.4	2.9	2.6	1.9	1.95	2.9	2.5
20*	1.0	1.4	1.3	2.1	1.45	2.1	1.6
21	4.1	2.8	3.2	3.5	3.40	4.1	3.6
22	2.1	1.6	2.4	3.2	2.33	3.2	2.6
23	6.3	6.9	6.0	6.0	6.30	6.9	6.4
24*	6.9	4.1	5.5	7.1	5.90	7.1	6.5
25	2.9	2.8	3.0	2.8	2.88	3.0	2.9
26	1.9	1.1	1.9	2.3	1.80	2.3	2.0
27	3.1	2.5	3.7	3.4	3.18	3.7	3.4
28	1.2	3.5	3.4	3.1	2.80	3.5	3.3
29	4.8	2.9	4.5	3.6	3.95	4.8	4.3
30	2.3	3.8	2.6	2.1	2.70	3.8	2.9
31	1.4	0.5	1.7	2.1	1.43	2.1	1.7
32	3.0	3.5	2.7	3.0	3.05	3.5	3.2
33	2.4	2.2	2.2	2.7	2.38	2.7	2.4
34	1.5	1.9	2.9	2.4	2.18	2.9	2.4
35	2.3	2.4	2.3	1.7	2.18	2.4	2.3
36	1.5	1.9	2.1	1.9	1.85	2.1	2.0

*Appropriate values from third replicate substituted for botched tests

Table B.4. Maximum Frame Entry burr measurements for second replicate (in experimental order)

Run	Frame (0.001") (4 orientations)				Mean	Max	Top 3
1	7.1	8.0	8.7	7.0	7.70	8.7	7.9
2	2.9	3.8	3.6	3.9	3.55	3.9	3.8
3	1.5	1.3	1.4	1.1	1.33	1.5	1.4
4	3.4	5.0	4.5	4.2	4.28	5.0	4.6
5	5.0	4.8	5.0	6.0	5.20	6.0	5.3
6	2.4	2.3	3.1	3.2	2.75	3.2	2.9
7	2.5	2.0	2.4	3.0	2.48	3.0	2.6
8	1.3	1.6	2.6	1.6	1.78	2.6	1.9
9	4.3	5.8	5.0	4.8	4.98	5.8	5.2
10	2.3	1.3	1.6	1.7	1.73	2.3	1.9
11	3.0	3.1	4.0	4.4	3.63	4.4	3.8
12	3.0	3.6	3.6	3.6	3.45	3.6	3.6
13	3.4	3.1	3.6	4.2	3.58	4.2	3.7
14	2.4	5.2	3.5	3.4	3.63	5.2	4.0
15	3.3	2.3	3.9	3.6	3.28	3.9	3.6
16	1.7	3.4	2.7	3.8	2.90	3.8	3.3
17	1.0	1.5	1.5	1.5	1.38	1.5	1.5
18	0.5	0.6	1.4	1.1	0.90	1.4	1.0
19	1.6	1.4	3.2	3.5	2.43	3.5	2.8
20	1.9	1.7	2.2	3.2	2.25	3.2	2.4
21	2.0	3.4	2.0	2.6	2.50	3.4	2.7
22	1.9	1.7	2.1	2.4	2.03	2.4	2.1
23	2.2	2.9	2.6	4.1	2.95	4.1	3.2
24	2.0	3.8	2.9	3.9	3.15	3.9	3.5
25	3.8	3.3	3.3	3.0	3.35	3.8	3.5
26	1.5	0.8	1.0	1.5	1.20	1.5	1.3
27	2.2	2.3	3.6	3.4	2.88	3.6	3.1
28	3.3	2.9	3.2	1.6	2.75	3.3	3.1
29	3.5	4.5	4.1		4.03	4.5	4.2
30*	2.4	3.0	3.3	2.6	2.83	3.3	3.0
31	1.1	1.2	1.3	1.8	1.35	1.8	1.4
32	1.0	1.5	0.8	1.4	1.18	1.5	1.3
33	1.1	2.1	1.7	2.1	1.75	2.1	2.0
34	1.2	1.5	1.1	2.0	1.45	2.0	1.6
35	1.1	1.8	1.9	2.9	1.93	2.9	2.2
36	2.6	1.7	2.3	1.7	2.08	2.6	2.2

*Appropriate values from third replicate substituted for botched tests

Table B.5. Average of top 3 optical comparator measurements of skin exit and frame entry burrs (sorted in order of original design)

Orig. Run	Skin Exit Burr (0.001")		Frame Entry Burr (0.001")	
	1st Rep.	2nd Rep.	1st Rep.	2nd Rep.
1	5.5	6.3	6.50	3.73
2	3.4	2.3	2.50	1.87
3	2.4	3.9	3.17	2.20
4	2.4	1.4	2.03	1.43
5	1.9	1.4	1.73	1.57
6	2.9	3.2	2.03	2.43
7	2.3	2.3	2.40	4.03
8	4.2	2.6	4.27	5.20
9	2.5	3.8	2.33	2.63
10	1.5	1.3	0.97	1.33
11	11.3	3.8	6.40	4.21
12	4.6	3.9	2.90	2.67
13	6.8	7.5	5.23	5.33
14	2.7	4.1	2.07	3.10
15	2.8	2.2	1.97	2.20
16	2.5	4.6	4.30	4.57
17	6.2	6.8	4.77	3.83
18	1.8	2.5	1.60	1.40
19	4.2	1.5	1.03	2.77
20	3.9	3.5	2.07	2.13
21	8.4	3.2	3.40	3.60
22	4.2	3.4	2.57	3.47
23	2.7	2.6	1.60	3.60
24	2.6	2.4	3.33	2.97
25	3.0	2.3	1.27	1.30
26	5.9	8.2	9.13	7.93
27	1.8	1.7	1.60	1.03
28	2.4	3.1	2.33	1.93
29	1.9	2.4	1.00	3.30
30	5.8	2.5	1.93	3.13
31	3.5	4.5	2.90	3.77
32	1.8	4.5	1.67	1.50
33	2.4	3.6	5.97	2.90
34	1.5	1.8	3.60	3.20
35	2.3	2.7	2.43	3.53
36	2.6	2.8	2.47	1.97

Table B.6. Post-drilling separation micrometer readings (0.001") (sorted in order of original design)

Orig. Run	1st Rep.	2nd Rep.
1	3	2.9
2	0.8	0.5
3	2.6	1
4	0.3	0.2
5	0.7	0.4
6	0	0.2
7	0.8	1.5
8	2.1	1.9
9	1.2	1.7
10	0.2	0.1
11	12.8	2.3
12	0.9	2
13	17.6	2.3
14	0.2	1
15	0.81	3
16	0.1	1.2
17	1.4	0.8
18	0.3	0.1
19	0.3	0.9
20	2.2	3.5
21	11.3	7.3
22	1.5	1.2
23	1.2	1.7
24	1.4	0.3
25	0.8	0.7
26	2.7	2.5
27	0.4	0.8
28	0	0.1
29	0.1	-0.1
30	7	7
31	2.7	2.5
32	1.5	0.2
33	0.6	1.4
34	1.7	0.4
35	0.6	2.3
36	2.3	2.6

Table B.7. Maximum and breakthrough thrust forces (sorted in order of original design)

	Max. Thrust Force (N)		Thrust Force at Breakthrough (N)	
Orig. Run	1st Rep.	2nd Rep.	1st Rep.	2nd Rep.
1	358*	287	353*	283
2	208	141	199	135
3	255	274	245	255
4	156	135	150	132
5	197	218	190	215
6	291	306	285	296
7	487	426	466	411
8	149	142	139	138
9	256	306	253	302
10	211	223	203	216
11	436	218	313	203
12	137	155	133	149
13	518	383	500	377
14	342	408	338	403
15	242	232	239	230
16	215	216	210	212
17	481	428	463	417
18	183	163	183	158
19	194	182	190	156
20	307	329	301	322
21	147	133	140	128
22	470	454	458	446
23	281	327	276	321
24	329	354*	323	345*
25	188	236	180	234
26	324	300	303	287
27	244*	272	241*	267
28	253	289	248	276
29	204	178	178	162
30	237	220	231	219
31	335	331	325	321
32	307	280	306	276
33	383	355	374	348
34	178	198	175	192
35	137	148	132	145
36	284	298	260	284

*Appropriate values from third replicate substituted for botched tests

APPEDIX C: Analysis

Table C.1. ANOVA for skin exit burr optical comparator readings

Source	DF	Seq SS	Adj SS	MS	F	P
A	1	6.191	1.037	1.037	0.46	0.498
B	**1**	**26.521**	**7.608**	**7.608**	**3.41**	**0.070**
C	1	0.755	0.015	0.015	0.01	0.935
D	2	12.431	9.218	4.609	2.07	0.136
E	**2**	**16.633**	**13.646**	**6.823**	**3.06**	**0.055**
F	2	5.982	4.43	2.215	0.99	0.377
G	**2**	**31.592**	**27.804**	**13.902**	**6.23**	**0.004**
H	**2**	**26.374**	**25.905**	**12.952**	**5.8**	**0.005**
I	1	0.854	0.854	0.854	0.38	0.539
Error	57	127.217	127.217	2.232		
Total	71	254.551				

Table C.2. ANOVA for frame entry burr optical comparator readings

Source	DF	Seq SS	Adj SS	MS	F	P
A	1	2.582	0.001	0.001	0	0.974
B	**1**	**17.739**	**14.692**	**14.692**	**11.8**	**0.001**
C	1	0.424	2.199	2.199	1.77	0.189
D	**2**	**31.705**	**28.123**	**14.062**	**11.3**	**0**
E	2	6.436	5.044	2.522	2.03	0.141
F	2	8.486	5.702	2.851	2.29	0.11
G	**2**	**20.688**	**18.067**	**9.033**	**7.27**	**0.002**
H	**2**	**21.25**	**20.617**	**10.308**	**8.29**	**0.001**
I	1	2.289	2.289	2.289	1.84	0.18
Error	57	70.85	70.85	1.243		
Total	71	182.449				

Table C.3. ANOVA for post-drilling separation micrometer readings

Source	DF	Seq SS	Adj SS	MS	F	P
A	1	2.492	0.216	0.216	0.03	0.853
B	**1**	**103.691**	**45.199**	**45.199**	**7.28**	**0.009**
C	1	4.089	3.123	3.123	0.5	0.481
D	2	0.247	4.329	2.164	0.35	0.707
E	2	5.825	1.584	0.792	0.13	0.881
F	2	34.11	29.431	14.715	2.37	0.103
G	**2**	**76.05**	**68.745**	**34.373**	**5.54**	**0.006**
H	**2**	**43.578**	**43.566**	**21.783**	**3.51**	**0.037**
I	1	1.381	1.381	1.381	0.22	0.639
Error	57	353.912	353.912	6.209		
Total	71	625.375				

Table C.2. ANOVA for breakthrough drilling thrust force

Source	DF	Seq SS	Adj SS	MS	F	P
A	**1**	**20965**	**10028**	**10028**	**5.72**	**0.02**
B	1	20682	253	253	0.14	0.705
C	**1**	**95741**	**36870**	**36870**	**21**	**0**
D	**2**	**110887**	**42723**	**21362**	**12.2**	**0**
E	**2**	**260529**	**229658**	**114829**	**65.5**	**0**
F	**2**	**8959**	**10882**	**5441**	**3.1**	**0.053**
G	2	7142	7381	3690	2.1	0.131
H	2	4572	4923	2462	1.4	0.254
I	1	3528	3528	3528	2.01	0.161
Error	57	99941	99941	1753		
Total	71	632945				